Estimation of Battery Internal Resistance Using Built-In Self-Scaling Method

Ai Hui Tan[a,*], Duu Sheng Ong[b] and Mathias Foo[c]

[a] Faculty of Engineering, Multimedia University, 63100 Cyberjaya, Malaysia; Email: htai@mmu.edu.my.

[b] Faculty of Engineering, Multimedia University, 63100 Cyberjaya, Malaysia; Email: dsong@mmu.edu.my.

[c] School of Engineering, University of Warwick, Coventry, CV4 7AL, United Kingdom;

Email: M.Foo@warwick.ac.uk.

[*] Corresponding author

Abstract

This paper proposes the use of the built-in self-scaling (BS) method for the effective estimation of the internal resistance of lithium-ion batteries. The internal resistance is a measure of the battery's state-of-health and an important parameter to monitor, especially in safety-critical applications such as hybrid electric vehicle applications. The BS technique works by identifying the system's impulse response and then computing the resistance from this response. This approach makes use of a prior DC gain which capitalizes on the fact that the state-of-health changes slowly with time. The BS method can be utilized on the fly in real time, is passive, and has high accuracy which is invariant with respect to the battery dynamics. Simulation results show that the BS method reduces the mean square error by factors of 32, 69 and 20 compared with the series resistance, the least squares and data pieces, and the kernel-based techniques, respectively, in the absence of hysteresis. The corresponding values in the presence of hysteresis are 42, 62 and 21, respectively. Experimental results using a lithium nickel manganese cobalt oxide battery and a dynamic current profile based on the Federal Urban Driving Schedule further confirm the superiority of the proposed BS approach.

Keywords: Hybrid electric vehicles; impulse response estimation; internal resistance estimation; lithium-ion batteries; state-of-health

Abbreviations

BMS: battery management system
BS: built-in self-scaling
ECM: equivalent circuit model
EIS: electrochemical impedance spectroscopy
FUDS: Federal Urban Driving Schedule
LD: least squares and data pieces
KB: kernel-based
MSE: mean square error
SNR: signal-to-noise ratio
SOC: state-of-charge
SOH: state-of-health
SR: series resistance

1. Introduction

Green technology, such as rechargeable battery technology, has drawn significant attention since the past few decades. The interest is spurred by the growing energy crisis and the urgency to reduce global warming by reducing carbon emissions. The encouraging uptake of electric vehicles and hybrid electric vehicles to replace petrol and diesel vehicles has provided a commercial case for improving battery technology since batteries form a key component of such green vehicles [1].

A favored choice of rechargeable battery is the lithium-ion battery. It has the advantages of outstanding specific energy and power, long calendar and cycle lives, high roundtrip efficiency and high reliability [2]. A disadvantage is that the battery requires an advanced battery management system (BMS) [2] since the modeling and prediction related to the battery are not trivial and depend on many factors, such as the state-of-charge (SOC) and temperature. An additional challenge is that a real battery is non-ideal and will age with time. Four lithium-ion battery technologies were compared under calendar aging in [3]; this work shows that different battery chemistries will lead to different aging characteristics. Regardless of a battery's chemistry, battery aging will affect its performance. To accurately predict a battery's performance and remaining lifetime, its state-of-health (SOH) must be determined [4]. This is particularly important for safety-critical applications since lithium is highly reactive and an incorrect estimate of the SOH may lead to serious negative consequences.

The impedance of a battery is a measure of its SOH. Several existing approaches on impedance measurement are based on impedance spectroscopy; see Section 2 for an overview. There are two major drawbacks. Firstly, the system must be allowed to reach equilibrium. The test is time-consuming and since the vehicle is typically not in equilibrium when it is in use, the estimation cannot be carried out on the fly. Secondly, the method is not passive, necessitating specialized test signals to be injected into the system. These signals include high frequency components that require fast sampling in the order of around 10kHz. Special equipment is needed, and the test cannot be performed when the vehicle is running. Note that a BMS typically has a sampling frequency in the order of around 1Hz [5].

There are passive techniques available for measuring the resistance of a battery, which is the real part of the impedance. These are the series resistance (SR) method [6] and a technique based on least squares and data pieces (LD) [7]. These methods require assumptions relating to the battery dynamics. The SR method assumes that the sampling frequency is relatively fast with respect to the system dynamics. The LD method assumes that the effects of diffusion voltages can be captured sufficiently using only one resistor-capacitor

pair. The dependence of the estimation accuracy on the battery dynamics is a shortcoming in these approaches.

The current work aims to propose a method to estimate the internal resistance of a lithium-ion battery, that is free from all the disadvantages mentioned above. The main contributions of this work are as follows:

(i) A built-in self-scaling (BS) method for measuring the internal resistance of a battery. The BS method can be utilized on the fly in real time, is passive, and has high accuracy which is invariant with respect to the battery dynamics.

(ii) Extensive simulations comparing the proposed approach with three different competing strategies. Results show that the proposed method is superior.

(iii) An application of the proposed BS method to real data measured from a battery. This illustrates the feasibility and effectiveness of the proposed approach.

The work is highly original due to the following:

(i) This is the first reported application of the BS method for measuring the internal resistance of a battery. The resistance is computed from the impulse response of the battery. This is a unique feature compared to existing methods.

(ii) The estimation problem is framed such that the slowly varying nature of the resistance is captured using the DC gain. This information is used in a novel way to reduce the fluctuations in the estimates, thus increasing their accuracy.

The rest of the paper is organized as follows. A literature review is presented in Section 2. The proposed BS technique is introduced in Section 3. Section 4 considers a detailed simulated case study. An application of the proposed BS method on experimental data measured from a battery is described in Section 5. Finally, concluding remarks and suggestions for future work are given in Section 6.

2. Literature Review

The impedance of a battery is typically modeled by an equivalent circuit model (ECM) [8]. An ECM of a battery cell (referred to simply as a battery for the rest of this paper) is shown in Fig. 1. V_{OCV} is the open circuit voltage which is a function of the SOC. In a BMS, the current i and the terminal voltage v are sampled at a sampling interval T. The relationship between the input $u = i$ and the output $y = V_{\mathrm{OCV}} - v$ can be expressed in the frequency domain (z-domain) as

$$\frac{Y(z)}{U(z)} = G(z) \tag{1}$$

where G is the internal impedance of the battery in the frequency domain (i.e., transfer function), and U and Y are the z-transforms of u and y, respectively.

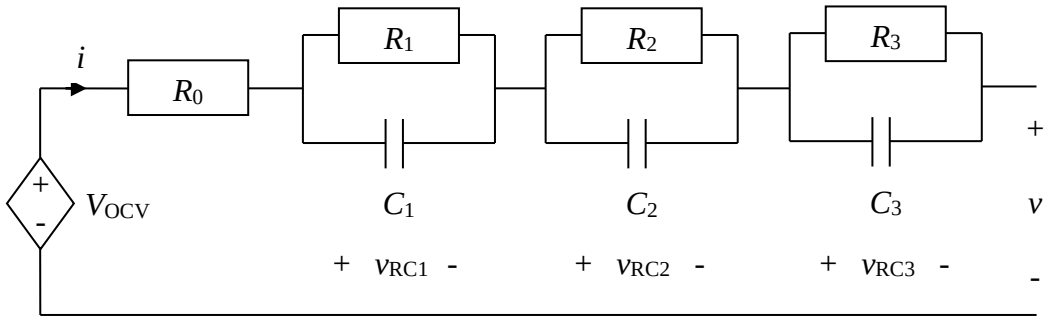

Fig. 1. Model of battery cell.

A popular method for estimating the battery SOH is via electrochemical impedance spectroscopy (EIS). It is suitable in cases where the battery can be disconnected from the load and taken to the laboratory for a test. In [9], the parameters of an ECM were extracted from the EIS data through nonlinear fitting. A relationship between the resistance and the available capacity was applied to evaluate the SOH. In [10], a fast impedance calculation-based battery SOH estimation method for lithium-ion battery was proposed from the perspective of the EIS. Some impedance features known as health factors were selected; these can indicate the aging of batteries. The SOH was evaluated using extreme machine learning with regularization. The relaxation effect on the SOH estimation when employing the EIS method was studied in [11]. A combination of fractional order impedance modeling and short-term relaxation effects was proposed. The EIS allows physical processes with different time constants and different frequency dependences to be decoupled [12]. It has an additional benefit that the mechanisms causing the aging can be revealed [13].

Broadband impedance spectroscopy is similar to the EIS, but instead of perturbing the system in a frequency-by-frequency manner using sinusoidal excitation, a single broadband excitation is used. Locorotondo et al. [14] utilized pseudorandom binary sequence excitation for measuring the battery impedance as these signals only require simple hardware and have low crest factors [15, 16]. A clustering method was shown to be effective in separating the different ranges of SOH. The use of broadband excitation was extended in [17, 18] to the application of direct synthesis ternary signals [19], which are capable of reducing the effects

of nonlinear distortion on the impedance measurement. Further to this, the Kronig-Kramers transformation test was employed to validate the uniqueness of the impedance spectra. Results show that the measured impedance is well compliant with the linearized ECM for SOH estimation.

The SR method tracks the resistance R_0. From Fig. 1, the rate of change of the v is given by

$$\frac{v_k - v_{k-1}}{T} = \frac{[V_{\mathrm{OCV},k} - i_k R_0 - v_{\mathrm{RC1},k} - v_{\mathrm{RC2},k} - v_{\mathrm{RC3},k} - (V_{\mathrm{OCV},k-1} - i_{k-1} R_0 - v_{\mathrm{RC1},k-1} - v_{\mathrm{RC2},k-1} - v_{\mathrm{RC3},k-1})]}{T} \tag{2}$$

where k is the discrete time index. The method assumes that V_{OCV} and the diffusion voltages v_{RC1}, v_{RC2} and v_{RC3} vary relatively slowly compared to i and v [6]. Thus, (2) can be simplified to

$$\frac{v_k - v_{k-1}}{T} \approx -R_0 \frac{i_k - i_{k-1}}{T}. \tag{3}$$

R_0 can be estimated at any sampling instant k from the change in v divided by the change in i. However, since $|i_k - i_{k-1}|$ may be small, R_0 is only re-estimated when $|i_k - i_{k-1}|$ exceeds a magnitude threshold M; otherwise, the previous estimate is maintained. (Based on the authors' observations, a relatively good performance can be obtained when M is set such that it is exceeded about half of the time.) Hence,

$$R_{0,k} = \begin{cases} -\dfrac{v_k - v_{k-1}}{i_k - i_{k-1}} & |i_k - i_{k-1}| > M \\ R_{0,k-1} & |i_k - i_{k-1}| \le M \end{cases} \tag{4}$$

and R_0 is averaged across k for a particular data record. The length of the data record depends on the required rate of update. Even though the SR approach can be applied in real time, the accuracy of the assumption relating to slow changes in the diffusion voltages may be of limited validity if the resistor and capacitor values of a particular pair are small, as this leads to a small time constant for that resistor-capacitor pair. The assumption is also of limited accuracy if the sampling frequency is relatively low compared to the system dynamics, since a lot can happen within a single sampling interval.

The LD method proposed in [7] provides a solution using least squares. It assumes that the ECM has only one resistor-capacitor pair. The key equation is

$$\frac{v_k - v_{k-1}}{T} = \begin{bmatrix} R_0 & \dfrac{R_0 + R_1}{R_1 C_1} & \dfrac{1}{R_1 C_1} & \dfrac{V_{\mathrm{OCV}}}{R_1 C_1} \end{bmatrix} \begin{bmatrix} -\dfrac{i_k - i_{k-1}}{T} & -i_k & -v_k & 1 \end{bmatrix}^T. \tag{5}$$

When V_{OCV} is known, (5) can be simplified to

$$\frac{v_k - v_{k-1}}{T} - \frac{V_{\mathrm{OCV}}}{R_1 C_1} = \theta^T \left[-\frac{i_k - i_{k-1}}{T} \quad -i_k \quad -v_k \right]^T \tag{6}$$

where $\theta^T = \left[R_0 \quad \frac{R_0 + R_1}{R_1 C_1} \quad \frac{1}{R_1 C_1} \right]$. This allows θ to be solved using least squares. Subsequently, $R_0 + R_1 = \theta_2 / \theta_3$.

3. Estimation of Internal Resistance using BS Method

In this work, it is proposed that the battery model (1) with $u = i$ and $y = V_{\mathrm{OCV}} - v$ be reformulated using the Bayesian estimation framework for impulse response estimation. In this framework, the system is a finite impulse response model described by

$$y_k = \sum_{i=0}^{k} u_{k-i} g_i + \varepsilon_k \tag{7}$$

where u_k, y_k and g_k are the input, output and impulse response, respectively. ε_k is the measurement (sensor) noise with a variance of σ^2. The impulse response $\mathbf{g} = \begin{bmatrix} g_0 & g_1 & \dots & g_{n-1} \end{bmatrix}^T$ is the inverse *z*-transform of *G*. Even though the impulse response is theoretically an infinite impulse response, it can in practice be truncated to a finite impulse response when the dynamics have sufficiently decayed below the noise level. This is because signal processing algorithms are unable to deal with an infinite impulse response as it will require infinite processing time and infinite memory.

In the Bayesian estimation framework, $\mathbf{g}$ has a probability distribution $\mathbf{g} \sim \mathcal{N}(\mathbf{0}_n, \mathbf{K})$, where $\mathcal{N}$ denotes the normal (Gaussian) distribution and $\mathbf{0}_n$ is the *n*-dimensional zero column vector. $\mathbf{K} \in \Re^{n \times n}$ is a positive definite prior covariance matrix. The kernel hyperparameters can be selected based on historical data or by using the Empirical Bayes method. The output $\mathbf{y} = \begin{bmatrix} y_0 & y_1 & \dots & y_{n-1} \end{bmatrix}^T$ is measured in synchrony with the input. For each processing, *N* samples forming one data record will be utilized. Some prior information on the battery dynamics should be available for the selection of suitable values of *N* and *n*. This is not restrictive in practice, because the characteristics of many different types of batteries are easily available from manufacturers. In a BMS, past input values (prior to the *N* samples in a

particular data record) are available allowing $\mathbf{U} = \begin{bmatrix} u_0 & u_{-1} & \cdots & u_{-(n-1)} \\ u_1 & u_0 & \cdots & u_{-(n-2)} \\ \vdots & \vdots & \ddots & \vdots \\ u_{N-2} & u_{N-3} & \cdots & u_{N-n-1} \\ u_{N-1} & u_{N-2} & \cdots & u_{N-n} \end{bmatrix}$ to be formed. It is further assumed that **y** has a normal distribution. Thus, **g** and **y** are jointly normal and can be expressed by the joint distribution

$$\begin{bmatrix} \mathbf{y} \\ \mathbf{g} \end{bmatrix} \sim \mathcal{N}\left(\begin{bmatrix} \mathbf{0}_N \\ \mathbf{0}_n \end{bmatrix}, \begin{bmatrix} \mathbf{U}\mathbf{K}\mathbf{U}^T + \sigma^2 \mathbf{I}_N & \mathbf{U}\mathbf{K} \\ \mathbf{K}\mathbf{U}^T & \mathbf{K} \end{bmatrix} \right) \tag{8}$$

where $\mathbf{I}_N$ denotes an identity matrix of size N. Using the property of conditional distribution, the posterior distribution of **g** is given by $\mathbf{g}|\mathbf{y} \sim \mathcal{N}(\hat{\mathbf{g}}, \hat{\mathbf{K}})$ [20] where

$$\hat{\mathbf{g}} = \frac{1}{\sigma^2}\hat{\mathbf{K}}\mathbf{U}^T\mathbf{y}\,,\ \hat{\mathbf{K}} = \left(\mathbf{K}^{-1} + \frac{1}{\sigma^2}\mathbf{U}^T\mathbf{U} \right)^{-1}. \tag{9}$$

Eq. (9) defines the standard kernel-based (KB) method for obtaining the estimated impulse response $\hat{\mathbf{g}}$.

In coming up with a new method for performing the estimation, it is useful to note that (i) the total resistance $R_{\text{total}} = R_0 + R_1 + R_2 + R_3$ changes slowly due to aging being a slow process (except in some special cases of sudden battery failure) and (ii) R_{total} is the DC gain of the impedance $G(z)$ as can be seen from Fig. 1. Thus the prior information on the DC gain can be capitalized upon in the estimation, which is exactly what the BS technique does. In the BS approach, the DC gain of the system is modeled by $s_\infty \sim \mathcal{N}(s_\infty^*, \sigma_\infty^2)$ where both s_∞^* and σ_∞^2 are known *a priori* [21]. In a BMS, s_∞^* can be easily set to the prior DC gain which is equal to the DC gain estimated from previous data records. Alternatively, it can also use any DC gain value from a calibration test if such a test has been conducted recently. The variance σ_∞^2 indicates the reliability of s_∞^*; this value can be selected based on the confidence in the value of s_∞^*. The actual value of the DC gain s_∞ is defined by $s_\infty = \sum_{k=0}^{n-1} g_k$. This is because the step function is the integral of the impulse function. In a similar way, the step response is the integral of the impulse response. In the discrete-time domain, the final value of the step response, i.e., the DC gain, can be computed by summing the impulse response.

Incorporating the DC gain term requires that **y** and **U** be modified to $\tilde{\mathbf{y}} = \begin{bmatrix} y_0 & y_1 & \dots & y_{N-2} & \eta s_\infty^* \end{bmatrix}^T$ and

$\tilde{\mathbf{U}} = \begin{bmatrix} u_0 & u_{-1} & \cdots & u_{-(n-1)} \\ u_1 & u_0 & \cdots & u_{-(n-2)} \\ \vdots & \vdots & \ddots & \vdots \\ u_{N-2} & u_{N-3} & \cdots & u_{N-n-1} \\ \eta & \eta & \cdots & \eta \end{bmatrix}$, with $\eta = \sqrt{\sigma^2/\sigma_\infty^2}$. Now, **g** and $\tilde{\mathbf{y}}$ are jointly normal and can be expressed by the joint distribution [21]

$$\begin{bmatrix} \tilde{\mathbf{y}} \\ \mathbf{g} \end{bmatrix} \sim \mathcal{N}\left(\begin{bmatrix} \begin{bmatrix} \mathbf{0}_{N-1} \\ \eta s_\infty^* \end{bmatrix} \\ \mathbf{0}_n \end{bmatrix}, \begin{bmatrix} \tilde{\mathbf{U}}\mathbf{K}\tilde{\mathbf{U}}^T + \sigma^2 \mathbf{I}_N & \tilde{\mathbf{U}}\mathbf{K} \\ \mathbf{K}\tilde{\mathbf{U}}^T & \mathbf{K} \end{bmatrix} \right). \tag{10}$$

Using the property of conditional distribution, the posterior distribution for the BS method is given by $\mathbf{g}|\tilde{\mathbf{y}} \sim \mathcal{N}(\hat{\mathbf{g}}, \hat{\mathbf{K}})$ where

$$\hat{\mathbf{g}} = \frac{1}{\sigma^2}\hat{\mathbf{K}}\tilde{\mathbf{U}}^T\tilde{\mathbf{y}}, \ \hat{\mathbf{K}} = \left(\mathbf{K}^{-1} + \frac{1}{\sigma^2}\tilde{\mathbf{U}}^T\tilde{\mathbf{U}} \right)^{-1}. \tag{11}$$

Note that the BS method does not require the system to be in equilibrium (steady-state). Finally, R_{total} is calculated from $R_{\text{total}} = \sum_{k=0}^{n-1} \hat{g}_k$. Additionally, the approach does not incur a high computational cost, as the matrices which require inversion are typically non-singular and of size $n \times n$, and n is usually not very large. It is thus suitable for use in BMS.

The method assumes that the values of V_{OCV}, SOC and temperature are available. Since these are monitored parameters in a BMS, this assumption is not restrictive. It is also known that R_1, R_2 and R_3 vary with SOC and temperature. The variation in R_{total} can be tracked based on its values in the past, which were measured under the same SOC and temperature conditions. For example, by using a data-logging system proposed in [22], the value of R_{total} at any point in time will only be compared to measurements made under the same conditions. Additionally, the proposed technique handles the effects of variation of resistances and capacitances with SOC, SOH and temperature by ensuring that the data record is short so that changes due to these effects are small. These ECM parameters are assumed to be constant across the data record; they can vary across different data records without introducing any problems to the BS technique. Note that the proposed approach does not require the individual values of the resistances and capacitances to be known. Importantly, the technique is independent of the ECM model. The hyperparameters of **K** can

be selected to achieve the desired bias-variance trade-off which is an advantage in this application.

4. Case Study

4.1. Simulation Settings

A performance comparison is carried out with $R_1 = 0.01\Omega$, $R_2 = 0.05\Omega$, $R_3 = 0.1\Omega$, $C_1 = 1\text{F}$, $C_2 = 5\text{F}$ and $C_3 = 10\text{F}$. These values are set based on some realistic values for resistance and capacitance in lithium-ion batteries [18]; note, however, that different battery chemistries may give different ECM parameter values. The sampling frequency is 2Hz, giving $T = 0.5\text{s}$. R_0 is set to increase from 0.02Ω to 0.04Ω across a time span of 10,000s. While this is a much faster increase compared to the rate of aging in practice, it is suitable for checking the performance of various methods in tracking the change in R_{total}. As an example, the impedance corresponding to $R_0 = 0.02\Omega$, truncated at $n = 15$, is given by $G(z) = 0.0965 + 0.0335z^{-1} + 0.0185z^{-2} + 0.0111z^{-3} + 0.0070z^{-4} + \ldots + 1.14\times10^{-4}z^{-14}$ with an impulse response $\mathbf{g} = \begin{bmatrix} 0.0965 & 0.0335 & \ldots & 1.14\times10^{-4} \end{bmatrix}^T$. This gives $R_{\text{total}} = 0.0965 + 0.0335 + \ldots + 1.14\times10^{-4} = 0.18\Omega$.

V_{OCV} is assumed to be fully known and is compensated for when computing y so its value is immaterial. In the simulation, the length of each data record is $N = 200$, corresponding to a time duration of 100s. This means that R_{total} is re-estimated every 100s, which is sufficiently fast since aging is a slow process. There are 110 data records in the simulation, corresponding to a total time of 11,000s. The first 10 data records are used to stabilize the system in order to provide some values of previous estimates to feed into the BS algorithm. These data records are subsequently discarded, leaving only 100 data records for comparison. The output additive white Gaussian noise variance σ^2 is set to 0.0126. (The unit is V^2, but this will be dropped for better readability.) This corresponds to a signal-to-noise ratio (SNR) of 30dB. Such an SNR is very reasonable and achievable for batteries for hybrid electric vehicle applications, as can be seen from the work described in [23], where the SNR was around 50dB. However, noting that the SNR will fluctuate when the vehicle is on the move, another set of tests at 10dB is also carried out with σ^2 increased to 1.26.

Four methods are compared, namely the SR, LD, KB and BS methods. For the SR method, only R_0 is estimated. To obtain R_{total} (so that the technique can be compared with the LD, KB and BS approaches), it is assumed that R_1, R_2 and R_3 are fully known for the SR

method. M is set to 5 and R_0 is initialized to the actual value. The LD technique is implemented with V_{OCV} assumed to be fully known. For the KB and BS methods, n is set to 15. This is sufficiently long for the system impulse response to have decayed. A tuned-correlated kernel is utilized. This kernel has only two hyperparameters to tune and is thus very practical for use in hybrid electric vehicle applications. As the system is time-varying, the hyperparameters are selected based on historical data. The kernel is chosen as $\mathbf{K}_{p,q} = 0.1 \times 0.7^{\max(p,q)}$. The DC gain for the BS method is set to $s_\infty^* = R_{\mathrm{total}}$ at the start of the simulation (for data record 1). This simulates the case in practice where the battery is calibrated in the laboratory at the beginning, middle and end of life points. Subsequent values of s_∞^* are obtained from an average of 10 previous estimated values. The value of σ_∞^2 is set to 1×10^{-5}, representing a rather high confidence on the estimated s_∞^*. η is set to 35.5 and this is fixed throughout the simulations.

A simulation is also carried out with all settings being the same as before but with instantaneous hysteresis nonlinearity being added. The hysteresis can describe the nonlinear changes in the cell voltage from V_{OCV}. These variations depend on whether the battery is charging or discharging. The hysteresis can be modeled by a relay function, with the current as the input [6]. In this simulation, it is described by

$$v_{\mathrm{hysteresis},k} = 0.04\,\mathrm{sgn}(i_k). \tag{12}$$

The hysteresis voltage is assumed to be unknown in all the methods being compared. Thus, there is no compensation for its effects; only the nominal constant value of V_{OCV} is compensated for. Note that dynamic hysteresis is not considered here, because the simulation does not take into account changes in the SOC.

4.2. Performance Comparison

The simulation is run 100 times which is adequate for studying the error characteristics because each run consists of 100 data points, giving a total of 10,000 data points from which the error statistics are derived. Results for the mean square error (MSE) $\mathrm{E}[(R_{\mathrm{total}} - \hat{R}_{\mathrm{total}})^2]$ and the variance of error $\mathrm{var}[R_{\mathrm{total}} - \hat{R}_{\mathrm{total}}]$ are summarized in Tables 1 and 2, where $\hat{R}_{\mathrm{total}}$ is the estimated value of R_{total} and E denotes the expectation operator. From Tables 1 and 2, it is clear that the BS method results in the lowest error values with and without hysteresis for SNRs of 30dB and 10dB. The large error of the SR method is due to two of the resistor-capacitor time constants being relatively small with respect to the

sampling interval, leading to an overestimate of R_{total}. The difference between the MSE and the variance of error is large for both the SR and LD techniques, indicating the presence of a significant bias. For the LD technique, the bias is due to the model mismatch caused by the assumption of a single resistor-capacitor pair. The estimates have a consistent bias in the form of an underestimate of 0.079Ω and 0.089Ω, respectively, for the cases with and without hysteresis. A small bias in the form of an underestimate of R_{total} also exists for the BS method, since the values of s_{∞}^{*} are obtained from an average of 10 previous estimated values when R_{total} is smaller (recalling that R_{total} increases with time).

Table 1. Error values of the various methods averaged from 100 runs, at an SNR of 30dB.

Method	Without hysteresis		With hysteresis	
	MSE	Variance of error	MSE	Variance of error
SR	3.18×10^{-3}	2.18×10^{-5}	4.05×10^{-3}	2.33×10^{-5}
LD	7.70×10^{-3}	3.50×10^{-5}	6.59×10^{-3}	3.55×10^{-5}
KB	4.19×10^{-5}	4.19×10^{-5}	8.40×10^{-5}	4.38×10^{-5}
BS	1.26×10^{-5}	2.97×10^{-6}	7.14×10^{-6}	1.89×10^{-6}

Table 2. Error values of the various methods averaged from 100 runs, at an SNR of 10dB.

Method	Without hysteresis		With hysteresis	
	MSE	Variance of error	MSE	Variance of error
SR	4.03×10^{-3}	8.60×10^{-4}	4.91×10^{-3}	8.61×10^{-4}
LD	7.74×10^{-3}	5.73×10^{-4}	6.69×10^{-3}	5.74×10^{-4}
KB	4.37×10^{-3}	4.38×10^{-3}	4.42×10^{-3}	4.38×10^{-3}
BS	2.13×10^{-4}	1.80×10^{-4}	2.08×10^{-4}	1.80×10^{-4}

The plots of the estimates are shown in Figs. 2 and 3, for SNRs of 30dB and 10dB, respectively, where it can be observed that the proposed BS method is superior under both SNRs. For all four methods, the estimated R_{total} is slightly higher when hysteresis is present. This is because the impedance model used by these techniques perceives the hysteresis voltage as being contributed by a larger total resistance. Based on the theory of best linear approximation [24], the nonlinear function (12) has a gain which depends on the amplitude distribution of the current in the battery. This gain causes the total resistance to "look larger".

Apparently, this is advantageous to the LD and BS methods as the MSE becomes smaller. This is due to an underestimate in R_{total} using these techniques. However, it is a disadvantage to the SR and KB methods as the SR method gives an overestimate in R_{total}, whereas the KB approach is largely unbiased.

Summarizing the results, the BS method is found on average to reduce the MSE by factors of 32, 69 and 20 compared with the SR, LD and KB techniques, respectively, in the absence of hysteresis. The corresponding values in the presence of hysteresis are 42, 62 and 21, respectively.

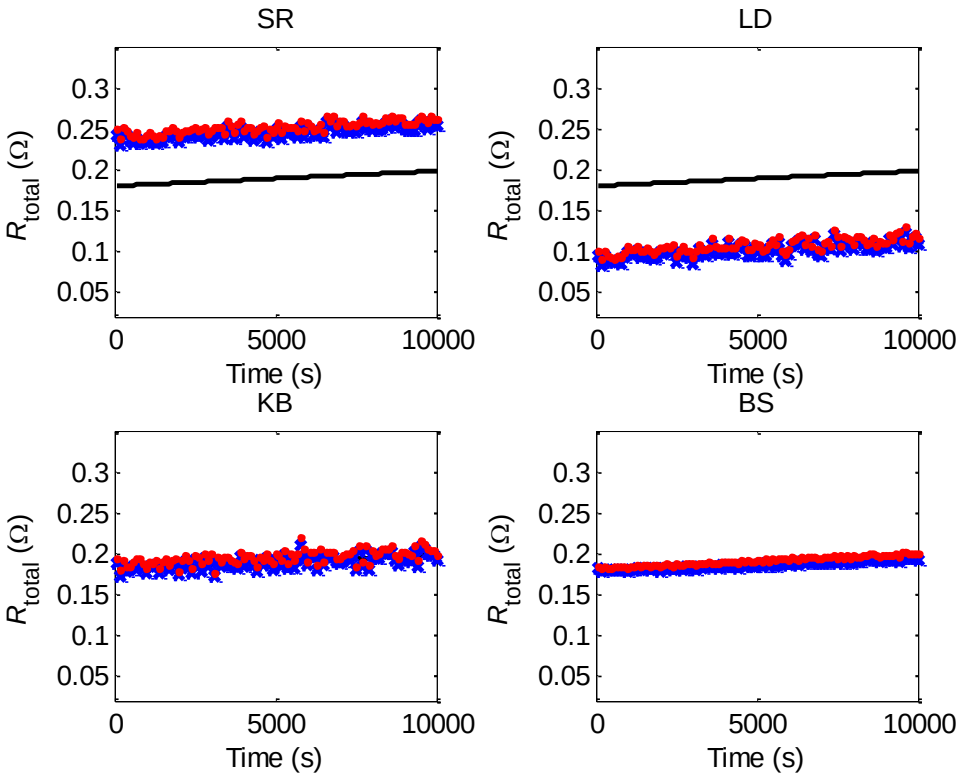

Fig. 2. Evolution of R_{total} against time for SNR of 30dB. Solid line: actual; blue crosses: estimates without hysteresis; red dots: estimates with hysteresis.

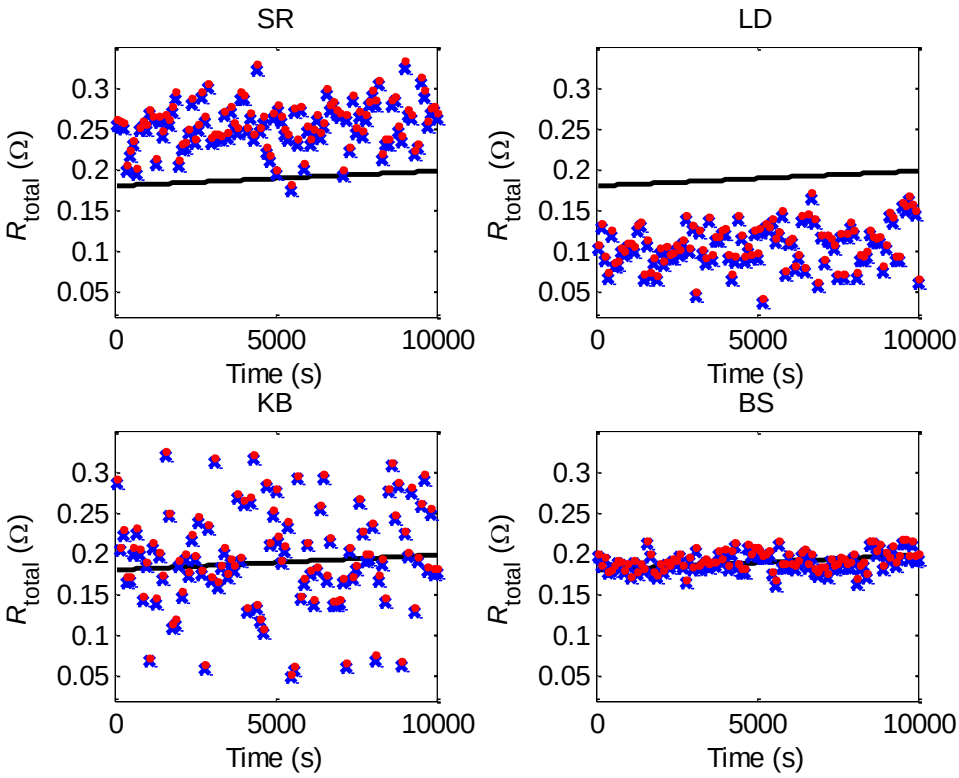

Fig. 3. Evolution of R_{total} against time for SNR of 10dB. Solid line: actual; blue crosses: estimates without hysteresis; red dots: estimates with hysteresis.

4.3. Estimation in the Presence of Open Circuit Voltage Inaccuracies

In practice, V_{OCV} is not exactly known but needs to be estimated by the BMS. Here, maintaining the settings described in Section 4.1, the estimation of R_{total} is carried out in the scenarios where V_{OCV} is underestimated and overestimated by 0.02V. The value of 0.02V corresponds to around 1.2% of the typical range of variation of V_{OCV}. This value is chosen based on [25], where the error in V_{OCV} when a simple ECM is used is around 0.02V; this is without temperature compensation in the model. Only constant underestimation and overestimation are considered, because the effects of a fluctuating error in V_{OCV} are the same as those of output noise which is already included in the simulation.

Results are summarized in Tables 3 and 4 for an SNR of 30dB. The performance of the SR and LD methods is hardly affected by the inaccuracies in V_{OCV}. The performance of the KB technique has deteriorated considerably compared to that in Table 1, whereas the BS approach shows a smaller deterioration. The BS method still gives the lowest error values for both the scenarios of underestimation and overestimation of V_{OCV}. Indeed, the MSE and variance of error values are significantly smaller than those of the competing techniques.

Results are summarized in Tables 5 and 6 for an SNR of 10dB, where it can be observed that all four techniques are largely unaffected by the inaccuracies in V_{OCV}. This is likely because the effects of noise have masked the effects of inaccurate V_{OCV}.

Table 3. Error values of the various methods averaged from 100 runs, at an SNR of 30dB, for underestimation of V_{OCV}.

Method	Without hysteresis		With hysteresis	
	MSE	Variance of error	MSE	Variance of error
SR	3.19×10^{-3}	2.16×10^{-5}	4.07×10^{-3}	2.31×10^{-5}
LD	7.72×10^{-3}	3.54×10^{-5}	6.60×10^{-3}	3.56×10^{-5}
KB	6.04×10^{-5}	6.04×10^{-5}	1.00×10^{-4}	6.21×10^{-5}
BS	1.43×10^{-5}	3.98×10^{-6}	7.76×10^{-6}	2.70×10^{-6}

Table 4. Error values of the various methods averaged from 100 runs, at an SNR of 30dB, for overestimation of V_{OCV}.

Method	Without hysteresis		With hysteresis	
	MSE	Variance of error	MSE	Variance of error
SR	3.17×10^{-3}	2.23×10^{-5}	4.05×10^{-3}	2.38×10^{-5}
LD	7.69×10^{-3}	3.46×10^{-5}	6.57×10^{-3}	3.49×10^{-5}
KB	5.96×10^{-5}	5.96×10^{-5}	9.94×10^{-5}	6.14×10^{-5}
BS	1.41×10^{-5}	3.68×10^{-6}	7.59×10^{-6}	2.70×10^{-6}

Table 5. Error values of the various methods averaged from 100 runs, at an SNR of 10dB, for underestimation of V_{OCV}.

Method	Without hysteresis		With hysteresis	
	MSE	Variance of error	MSE	Variance of error
SR	4.01×10^{-3}	8.48×10^{-4}	4.90×10^{-3}	8.50×10^{-4}
LD	7.67×10^{-3}	5.62×10^{-4}	6.63×10^{-3}	5.62×10^{-4}
KB	4.19×10^{-3}	4.18×10^{-3}	4.23×10^{-3}	4.18×10^{-3}
BS	2.11×10^{-4}	1.74×10^{-4}	2.04×10^{-4}	1.72×10^{-4}

Table 6. Error values of the various methods averaged from 100 runs, at an SNR of 10dB, for overestimation of V_{OCV}.

Method	Without hysteresis		With hysteresis	
	MSE	Variance of error	MSE	Variance of error
SR	4.01×10^{-3}	8.67×10^{-4}	4.89×10^{-3}	8.69×10^{-4}
LD	7.72×10^{-3}	5.61×10^{-4}	6.68×10^{-3}	5.61×10^{-4}
KB	4.21×10^{-3}	4.21×10^{-3}	4.26×10^{-3}	4.21×10^{-3}
BS	2.00×10^{-4}	1.72×10^{-4}	1.97×10^{-4}	1.71×10^{-4}

4.4. Variation of Estimation Accuracy with Parameter Changes

In Section 4.2, the results are shown for the case where the battery is modeled using three resistor-capacitor pairs. It is of interest to investigate the scenario where a single resistor-capacitor pair is sufficient for modeling a particular battery. This is also in line with some existing literature which assumes a single resistor-capacitor pair such as [26], and notably [7], which proposes the LD technique. Indeed, for estimation methods which rely on the ECM, a first order model with a single resistor-capacitor pair is recommended due to the trade-off between estimation accuracy and model complexity [27]. However, since the proposed BS method does not rely on the ECM, no such complexity constraint exists when using the BS method.

In the first experiment, R_0 is set to increase from 0.02Ω to 0.04Ω as before, R_1 = 0.05Ω and C_1 is varied. Results are plotted in Figs. 4 and 5, where each point is computed from a total of 10,000 values (100 points per run and 100 runs). Some important observations can be made as follows. The MSE for the SR method decreases as C_1 increases, as the system time constant becomes larger. For the LD method, the MSE and variance are much smaller than those obtained in Section 4.2 because the model with a single resistor-capacitor pair matches that used in the algorithm to compute the resistance. However, the error increases with C_1 because a larger C_1 corresponds to a larger time constant and a slower system response. Since the quantity of interest is R_{total} which is the impedance at steady-state, a faster system response will give a more accurate estimate for the LD technique. However, this is not the case for the SR method because the SR method only estimates R_0 and the actual value of R_1 is added to it to give the estimated R_{total}. Thus, a slow system response is favorable to the SR method, but the opposite effect is observed for the LD method.

It is interesting to note that the change in C_1 has little effect on the variance. Additionally, both the KB and BS approaches are not affected by the value of C_1. These approaches are also equally effective for the model with a single resistor-capacitor pair as for the model with three resistor-capacitor pairs, with the errors being comparable in both scenarios. The presence of hysteresis is favorable towards the LD and BS techniques because it reduces the bias (underestimate) in R_{total}. The opposite is true for the SR and KB methods, similar to the observation in Section 4.2, because there is negligible bias in the KB estimate whereas the SR approach leads to an overestimate. The BS method again results in the lowest MSE and variance of error among the four methods tested.

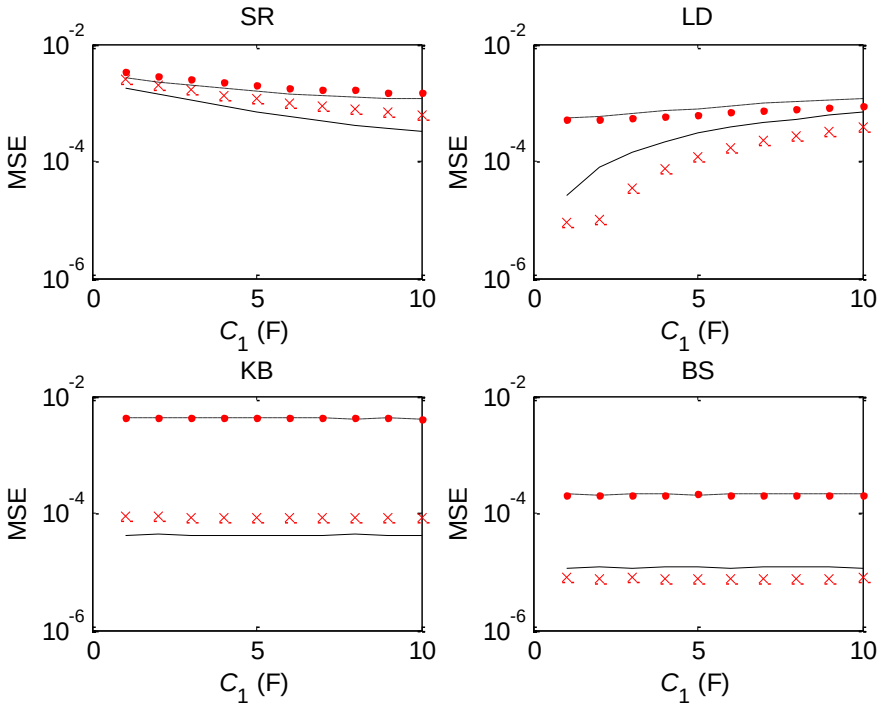

Fig. 4. Changes of MSE with C_1 when R_1 = 0.05Ω. Black solid line: SNR of 30dB without hysteresis; red crosses: SNR of 30dB with hysteresis; black dashed line: SNR of 10dB without hysteresis; red dots: SNR of 10dB with hysteresis.

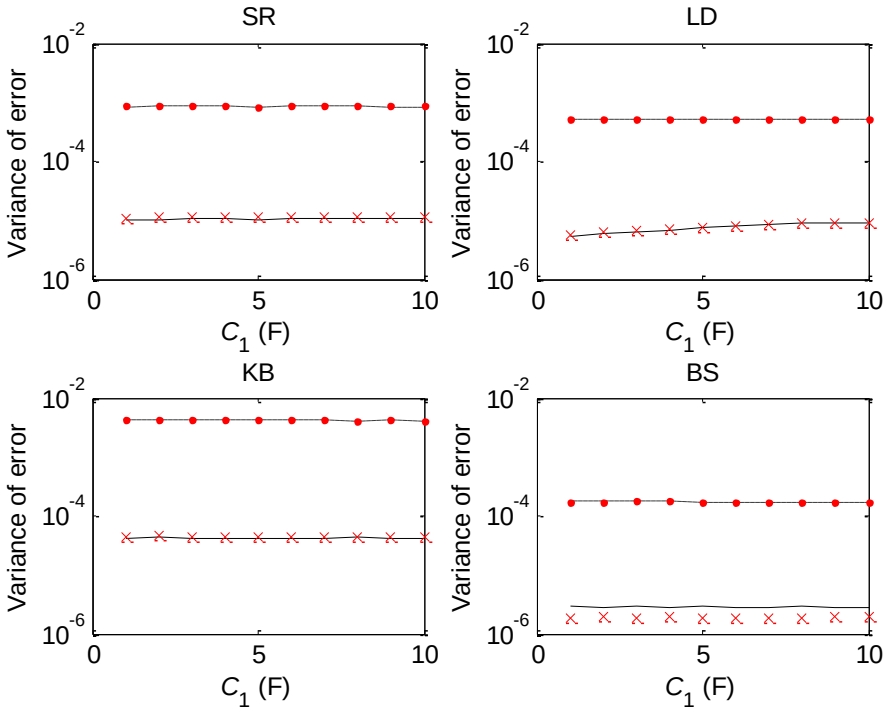

Fig. 5. Changes of variance of error with C_1 when R_1 = 0.05Ω. Black solid line: SNR of 30dB without hysteresis; red crosses: SNR of 30dB with hysteresis; black dashed line: SNR of 10dB without hysteresis; red dots: SNR of 10dB with hysteresis.

In the second experiment, R_0 is set to increase from 0.02Ω to 0.04Ω as before, C_1 = 5F and R_1 is varied from 0.01Ω to 0.1Ω. The performance is compared in Figs. 6 and 7. The MSE of the SR technique increases with R_1. Even though this gives a slower system response, a larger R_1 leads to a larger gain and a correspondingly larger error term. The LD method has MSE which generally increases with R_1 although the trend is slightly different when hysteresis is present. It is important to note that the proposed BS technique achieves the lowest MSE and variance of error. Additionally, it has a significant advantage that the estimation accuracy does not depend on the values of R_1 and C_1 as well as the number of resistor-capacitor pairs in the battery model. This advantage is also applicable to the KB method.

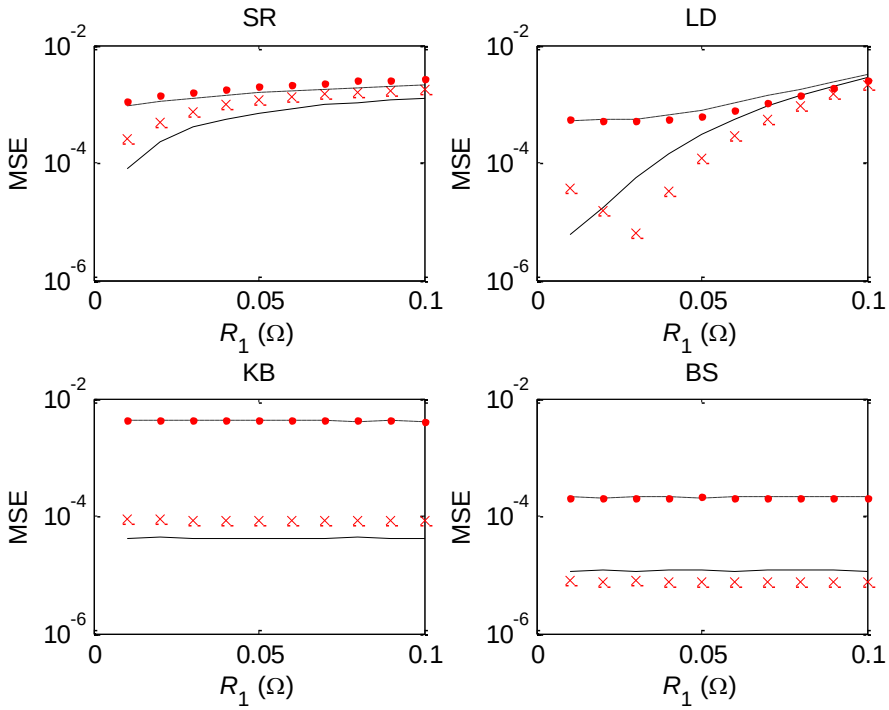

Fig. 6. Changes of MSE with R_1 when C_1 = 5F. Black solid line: SNR of 30dB without hysteresis; red crosses: SNR of 30dB with hysteresis; black dashed line: SNR of 10dB without hysteresis; red dots: SNR of 10dB with hysteresis.

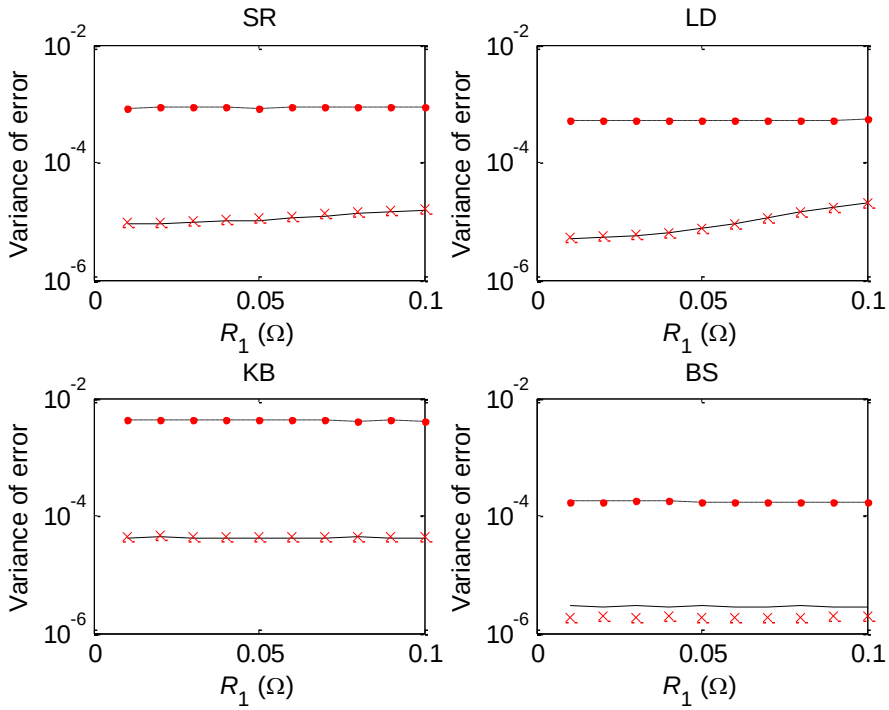

Fig. 7. Changes of variance of error with R_1 when C_1 = 5F. Black solid line: SNR of 30dB without hysteresis; red crosses: SNR of 30dB with hysteresis; black dashed line: SNR of 10dB without hysteresis; red dots: SNR of 10dB with hysteresis.

5. Application Example

5.1. Description of Dataset

Data were obtained from the CALCE Battery Research Group, University of Maryland, USA [27]. In particular, the battery used in this experiment is a cylindrical cell INR 18650-20R which is a lithium nickel manganese cobalt oxide battery. It has a capacity rating of 2000mAh, a nominal voltage of 3.6V, a lower cut-off voltage of 2.5V and an upper cut-off voltage of 4.2V.

The dataset was collected using a dynamic current profile based on the Federal Urban Driving Schedule (FUDS) as the input excitation signal. The FUDS is a dynamic electric vehicle performance test based on a time-velocity profile from an automobile industry standard vehicle [28]. It emulates an urban driving profile and is more complex than a dynamical stress testing profile in terms of the changing rate of the current [29]. The data were measured with the battery starting at an SOC of 80% and a temperature of 25°C. The temperature was maintained constant at 25°C throughout the experiment, but the SOC decreased continuously until it reached around 10%. The sampling interval was 1s.

There are eight periods in the dataset. In the current paper, three of the periods are considered for better clarity of presentation; these are periods 3, 4 and 5 in the dataset and they have SOCs of approximately 60% to 30%. The three periods are plotted in Fig. 8.

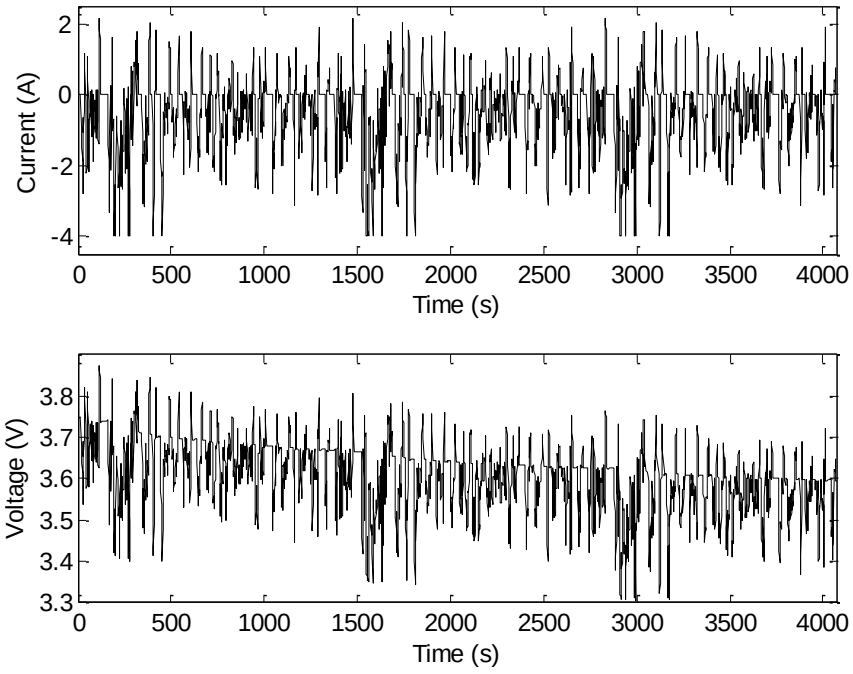

Fig. 8. Input and output data for INR 18650-20R based on the FUDS profile.

5.2. Offline System Identification

Each period of data is processed as follows. The mean values are removed from the data as is the normal practice in system identification [30]. The trend in the data is also removed to minimize the effects of decreasing V_{OCV}, since V_{OCV} is not estimated by the model. Linear system identification is utilized, without any knowledge of the mapping between V_{OCV} and SOC. The first 70% of each period is used as the training set, whereas the last 30% is used as the validation set. This avoids overfitting of the data. The fit is defined by $100\times\left(1-\sqrt{\frac{\sum_k (y_k-\hat{y}_k)^2}{\sum_k y_k^2}}\right)$%, where $\hat{y}$ denotes the estimated output. The results obtained using different model orders are shown in Table 7.

Table 7. Fit (in %) for different model orders.

Order	1	2	3	4	5
Period 3	88.53	91.02	93.89	94.51	94.45
Period 4	92.04	94.43	95.06	95.71	96.29
Period 5	92.84	96.30	96.49	96.69	96.92

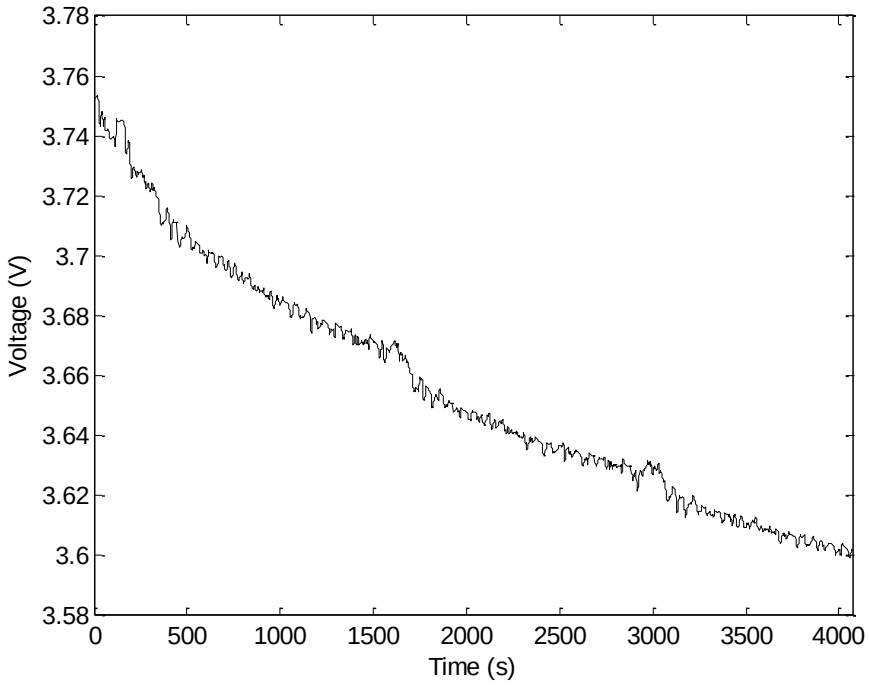

Fig. 9. Combined effect of V_{OCV} and $v_{hysteresis}$.

Based on Table 7, a second order model seems to be sufficient since the fit for third order models is only marginally better. The increase in the fit from order 1 to order 2 is quite significant. Hence, a second order model is used to estimate the system output for the purpose of subsequently estimating the unknown V_{OCV} plus the voltage due to hysteresis. The resulting error $y_k - \hat{y}_k$ is filtered using a fifth order model to give an estimate of V_{OCV} plus the voltage due to hysteresis. This voltage is plotted in Fig. 9. Note that this voltage is estimated entirely offline, as the purpose of the current work is not V_{OCV} estimation, but the values are required for the calculation of the resistance. A standard BMS would incorporate an algorithm to estimate V_{OCV} online. A summary of the steps in the offline identification is depicted in Fig. 10.

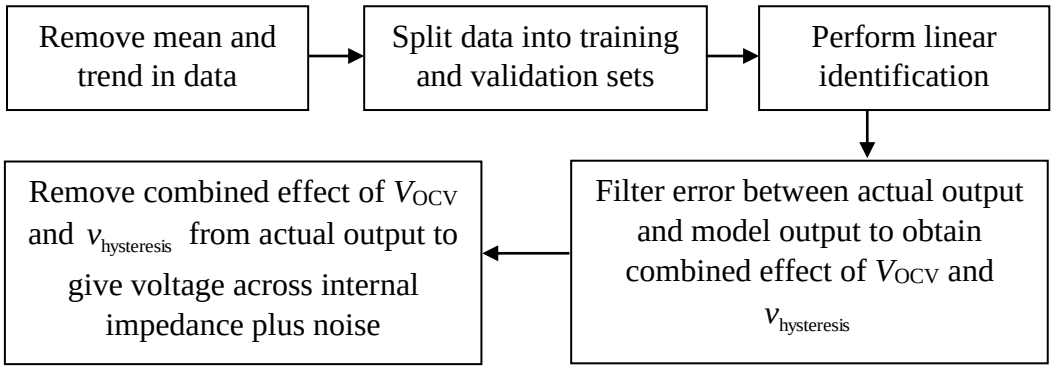

Fig. 10. Summary of the steps in the offline identification.

5.3. Online Estimation of Internal Resistance

Online estimation of internal resistance is carried out using the SR, LD, KB and BS approaches. The data record is chosen as N = 100, corresponding to a time duration of 100s. There are 40 data records across the three periods tested. It is important to note that the SR method estimates R_0 whereas the LD, KB and BS techniques estimate R_{total}.

For the SR method, M is set to 0.3 and R_0 is initialized to 0.071Ω. The LD method is performed assuming that V_{OCV} is available, as this was estimated in Section 5.2. For the KB and BS techniques, n is chosen to be 100 since the system dynamics are rather slow and there is a limitation that $n \leq N$. The kernel is chosen as $\mathbf{K}_{p,q} = 2 \times 0.7^{\max(p,q)}$, with $\sigma^2 = 0.01$. For the BS method, the first 10 data records are initialized using an inaccurate value of R_{total} with s_∞^* = 0.1. Subsequent values of s_∞^* are obtained from an average of 10 previous estimated values.

The value of σ_∞^2 is set to 5×10^{-3} for the first 10 data records as the guess of the DC gain is not with a high confidence initially. However, from data record 11 onwards, σ_∞^2 is set to 1×10^{-5}, representing a rather high confidence on the estimated s_∞^*.

The performance of the four methods is illustrated in Fig. 11. The solid lines refer to the resistances R_0 and R_{total} estimated using the low-current open circuit voltage method in [27]; this method is not a passive method. The method was implemented using a specialized input injection on the same battery. Thus, the resulting values (R_0 = 0.0710Ω and R_{total} = 0.0932Ω) are themselves estimates, and no theoretical values are available. However, the closeness of the SR estimate with R_0 = 0.0710Ω and the closeness of the BS estimate with R_{total} = 0.0932Ω give confidence in the results obtained. The initial fluctuations in the BS approach are due to the values in $\tilde{\mathbf{U}}$ being incomplete as the previous data records are not available at the start of the simulation and also that s_∞^* is started with an incorrect guess. Subsequent estimates are much smoother compared with the estimates from the LD and KB techniques, after the fluctuations have decayed. At the end of the experiment corresponding to the last data record, the BS method has an estimated impedance $\hat{G}(z) = 0.0720 + 0.0021z^{-1} + 0.0007z^{-2} + 0.0012z^{-3} + 0.0010z^{-4} + \ldots + 2.53\times10^{-13}z^{-99}$ with an estimated impulse response $\hat{\mathbf{g}} = \begin{bmatrix} 0.0720 & 0.0021 & \ldots & 2.53\times10^{-13} \end{bmatrix}^T$. This gives $R_{\text{total}} = 0.0720 + 0.0021 + \ldots + 2.53\times10^{-13} = 0.0930\Omega$. It is also worth noting that the relatively slow dynamics and the low model order ensure that the SR and LD approaches lead to relatively good estimates.

The mean and variance of the estimates are shown in Table 8. These are computed from data records 11 to 40, after the fluctuations have decayed. It can be seen that the variance of the BS approach is the smallest among the four methods tested. It is in fact more than a factor of two smaller than that of its closest competitor, which is the SR method. The mean value of the BS estimate is very close to R_{total} = 0.0932Ω. However, since the values from the low-current open circuit voltage method are not theoretical values and the actual resistances may themselves vary slightly across the experiment due to changes in the SOC, no MSE and variance of error are computed. This application example on a real battery effectively illustrates the potential impact of the proposed BS method for real-time monitoring of SOH through the estimation of the internal resistance.

Table 8. Mean and variance of the estimates using the FUDS profile.

Method	Mean of estimate	Variance of estimate
SR	0.0708	1.11×10^{-7}
LD	0.0929	6.38×10^{-6}
KB	0.0920	4.77×10^{-6}
BS	0.0931	4.76×10^{-8}

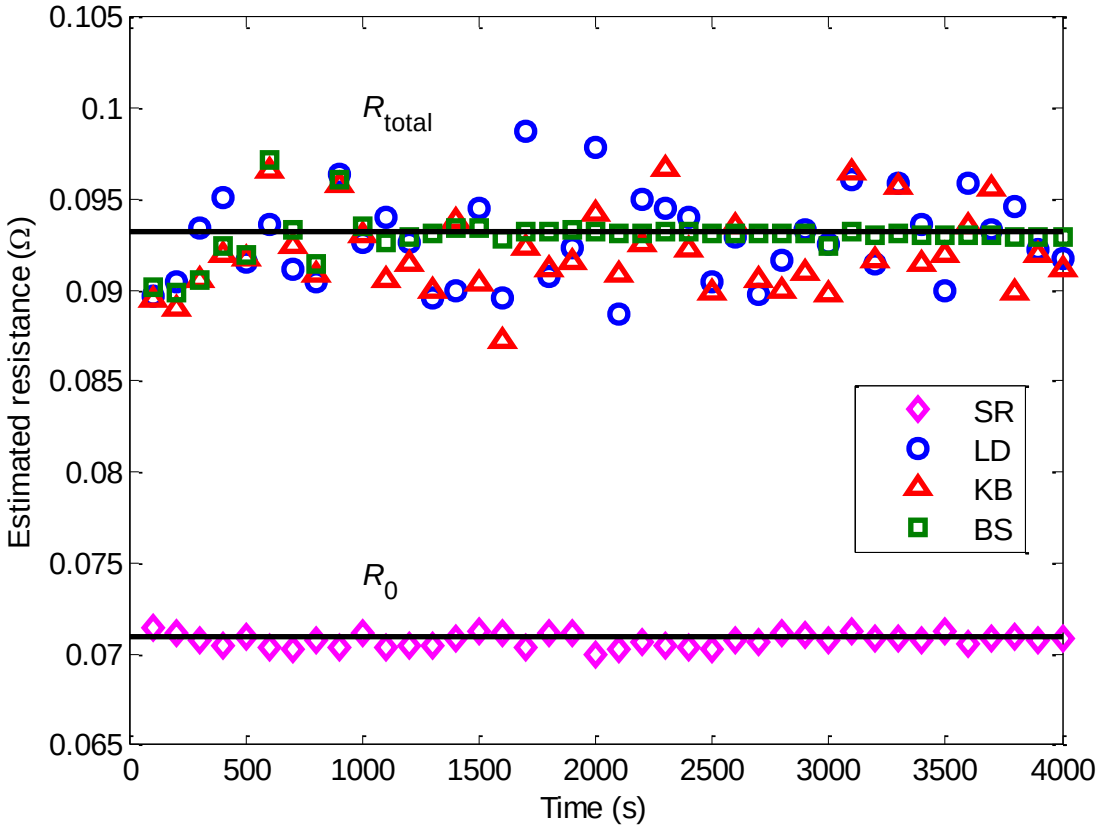

Fig. 11. Estimated resistance using the FUDS profile. The black solid lines correspond to R_0 and R_{total} estimated using the low-current open circuit voltage method in [27].

6. Conclusions

The BS method for real-time estimation of battery internal resistance is proposed. The method is a passive method that does not require special excitation signals. It is shown that the BS approach achieves smaller MSE and variance of error compared with its SR, LD and KB counterparts under different noise levels as well as in the presence and absence of hysteresis. The superior performance is maintained when the open circuit voltage is incorrectly estimated. Additionally, the technique works equally well for different battery

dynamics, both in terms of the time constants as well as the number of resistor-capacitor pairs required for modeling the system. An application example on a real battery using a dynamic current profile from an automobile industry standard vehicle illustrates the effectiveness of the BS method over the SR, LD and KB methods for hybrid electric vehicle applications.

Suggestions for future work include testing the BS method for different lithium-ion battery technologies as well as for applications with different typical current profiles, such as smartphones.

Acknowledgment

The authors would like to thank the Center for Advanced Life Cycle Engineering (CALCE) Battery Group, University of Maryland, USA, for making available the dataset used in this work.

Funding

This research did not receive any specific grant from funding agencies in the public, commercial, or not-for-profit sectors.

References

[1] N. Noura, L. Boulon, S. Jemeï, A review of battery state of health estimation methods: Hybrid electric vehicle challenges, World Electric Vehicle Journal, 11 (2020) DOI: 10.3390/wevj11040066.

[2] G. Zubi, R. Dufo-López, M. Cavalho, G. Pasaoglu, The lithium-ion battery: State of the art and future perspectives, Renewable and Sustainable Energy Reviews, 89 (2018) 292–308.

[3] A. Eddahech, O. Briat, J.-M. Vinassa, Performance comparison of four lithium-ion battery technologies under calendar aging, Energy, 84 (2015) 542–550.

[4] K.S.R. Mawonou, A. Eddadech, D. Dumur, D. Beauvois, E. Godoy, State-of-health estimators coupled to a random forest approach for lithium-ion battery aging factor ranking, Journal of Power Sources, 484 (2021), 229154.

[5] S. Yang, Y. Cao, S. Zhou, Y. Hua, X. Zhou, X. Liu, A comprehensive evaluation on variable sampling intervals of power battery system for electric vehicles, IEEE Access, 8 (2020) 156232–156243.

[6] G.L. Plett, Battery Management Systems: Equivalent-Circuit Methods, Artech House, Norwood, USA, 2016.

[7] J. Fan, Y. Zou, X. Zhang, Quantifying electric vehicle battery's ohmic resistance increase caused by degradation from on-board data, IFAC PapersOnLine, 52 (2019) 297–302.
[8] J. Sihvo, T. Roinila, D.-I. Stroe, Novel fitting algorithm for parameterization of equivalent circuit model of Li-ion battery from broadband impedance measurements, IEEE Transactions on Industrial Electronics, 68 (2021) 4916–4926.
[9] M. Galeotti, L. Cinà, C. Giammanco, S. Cordiner, A. Di Carlo, Performance analysis and SOH (state of health) evaluation of lithium polymer batteries through electrochemical impedance spectroscopy, Energy, 89 (2015) 678–686.
[10] Y. Fu, J. Xu, M. Shi, X. Mei, A fast impedance calculation based battery state-of-health estimation method, IEEE Transactions on Industrial Electronics, 69 (2021) 7019–7028.
[11] M. Messing, T. Shoa, S. Habibi, Estimating battery state of health using electrochemical impedance spectroscopy and the relaxation effect, Journal of Energy Storage, 43 (2021), 103210.
[12] S. Cruz-Manzo, P. Greenwood, An impedance model based on a transmission line circuit and a frequency dispersion Warburg component for the study of EIS in Li-ion batteries, Journal of Electroanalytical Chemistry, 871 (2020), 114305.
[13] J. Liu, Q. Duan, L. Feng, M. Ma, J. Sun, Q. Wang, Capacity fading and thermal stability of $LiNi_xCo_yMn_zO_2$/graphite battery after overcharging, Journal of Energy Storage, 29 (2020), 101397.
[14] E. Locorotondo, V. Cultrera, L. Pugi, L. Berzi, M. Pierini, G. Lutzemberger, Development of a real-time battery state of health diagnosis based on fast impedance measurements, Journal of Energy Storage, 38 (2021), 102566.
[15] A.H. Tan, K.R. Godfrey, The generation of binary and near-binary pseudorandom signals: An overview, IEEE Transactions on Instrumentation and Measurement, 51 (2002) 583–588.
[16] A.H. Tan, K.R. Godfrey, Industrial Process Identification: Perturbation Signal Design and Applications, Springer, Cham, Switzerland, 2019.
[17] J. Sihvo, T. Roinila, D.-I. Stroe, Broadband impedance measurement of lithium-ion battery in the presence of nonlinear distortions, Energies, 13 (2020), 2493.
[18] J. Sihvo, SOH estimation of Li-ion batteries based on broadband impedance measurements and equivalent circuit model analysis, Ph.D. Thesis, Tampere University of Technology, Finland, 2021.
[19] A.H. Tan, Direct synthesis of pseudo-random ternary perturbation signals with harmonic multiples of two and three suppressed, Automatica, 49 (2013) 2975–2981.

[20] C.E. Rasmussen, C.K.I. Williams, Gaussian Processes for Machine Learning, MIT Press, Cambridge, USA, 2006.
[21] A.H. Tan, D.S. Ong, Kernel-based impulse response estimation with prior DC gain using built-in self-scaling technique, IEEE Transactions on Instrumentation and Measurement, 69 (2020) 7295–7305.
[22] A.O. Tessier, M.R. Dubois, J.P. Trovão, Real-time estimator Li-ion cells internal resistance for electric vehicle application, World Electric Vehicle Journal, 8 (2016) 410–421.
[23] R. Relan, T. Koen, J.-M. Timmermans, J. Schoukens, A local polynomial approach to nonparametric estimation of the best linear approximation of lithium-ion battery from multiple datasets, IEEE Control Systems Letters, 1 (2017) 182–187.
[24] M. Enqvist, L. Ljung, Linear approximations of nonlinear FIR systems for separable input processes, Automatica, 41 (2005) 459–473.
[25] Y. Xing, W. He, M. Pecht, K.W. Tsui, State of charge estimation of lithium-ion batteries using the open-circuit voltage at various ambient temperatures, Applied Energy, 113 (2014) 106–115.
[26] H. He, R. Xiong, H. Guo, Online estimation of model parameters and state-of-charge of $LiFePO_4$ batteries in electric vehicles, Applied Energy, 89 (2012) 413–420.
[27] F. Zheng, Y. Xing, J. Jiang, B. Sun, J. Kim, M. Pecht, Influence of different open circuit voltage tests on state of charge online estimation for lithium-ion batteries, Applied Energy, 183 (2016) 513–525.
[28] United States Advanced Battery Consortium, Electric Vehicle Battery Test Procedures Manual, 1996.
[29] W. He, N. Williard, C. Chen, M. Pecht, State of charge estimation for Li-ion batteries using neural network modeling and unscented Kalman filter-based error cancellation, Electrical Power and Energy Systems, 62 (2014) 783–791.
[30] R. Pintelon, J. Schoukens, System Identification: A Frequency Domain Approach, John Wiley & Sons, Inc., Hoboken, USA, 2012.